

# Impact of Acute Ocular Hypertension on Retinal Ganglion Cell Loss in Mice

Meng Xuan<sup>1</sup>, Wei Wang<sup>1</sup>, Gabriella Bulloch<sup>2,3</sup>, Jian Zhang<sup>1</sup>, Jason Ha<sup>2</sup>, Qilin Wang<sup>1</sup>, Juanjuan Wang<sup>1</sup>, Xingyan Lin<sup>1</sup>, and Mingguang He<sup>1,4-6</sup>

<sup>1</sup> State Key Laboratory of Ophthalmology, Zhongshan Ophthalmic Center, Sun Yat-Sen University, Guangdong Provincial Key Laboratory of Ophthalmology and Visual Science, Guangzhou, Guangdong, China

<sup>2</sup> Centre for Eye Research Australia, Royal Victorian Eye and Ear Hospital, East Melbourne, Victoria, Australia

<sup>3</sup> Faculty of Science, Medicine and Health, University of Melbourne, Melbourne, Victoria, Australia

<sup>4</sup> School of Optometry, The Hong Kong Polytechnic University, Kowloon, Hong Kong, China

<sup>5</sup> Research Centre for SHARP Vision (RCSV), The Hong Kong Polytechnic University, Kowloon, Hong Kong, China

<sup>6</sup> Centre for Eye and Vision Research (CEVR), Hong Kong, China

**Correspondence:** Mingguang He, Centre for Eye and Vision Research (CEVR), 17W Hong Kong Science Park, Hong Kong School of Optometry, The Hong Kong Polytechnic University, Kowloon, 11 Yuk Choi Road, Hung Hom, KLN, Hong Kong 3002, China. e-mail: [mingguang.he@polyu.edu.hk](mailto:mingguang.he@polyu.edu.hk)

**Received:** May 2, 2023

**Accepted:** February 7, 2024

**Published:** March 20, 2024

**Keywords:** retinal ganglion cell; acute ocular hypertension; intraocular pressure; duration; yellow fluorescent protein

**Citation:** Xuan M, Wang W, Bulloch G, Zhang J, Ha J, Wang Q, Wang J, Lin X, He M. Impact of acute ocular hypertension on retinal ganglion cell loss in mice. *Transl Vis Sci Technol.* 2024;13(3):17, <https://doi.org/10.1167/tvst.13.3.17>

**Purpose:** To assess the correlation between intraocular pressure (IOP) levels and retinal ganglion cell (RGC) loss across different fixed-duration episodes of acute ocular hypertension (AOH).

**Methods:** AOH was induced in Thy1-YFP-H transgenic mice by inserting a needle connected to a saline solution container into the anterior chamber. Thirty-one groups were tested, each comprising three to five mice exposed to IOP levels ranging from 50 to 110 mm Hg in 5/10 mm Hg increments for 60/90/120 minutes and a sham control group. The YFP-expressing RGCs were quantified by confocal scanning laser ophthalmoscopy, whereas peripapillary ganglion cell complex thickness was measured using spectral-domain optical coherence tomography. Changes in RGC count and GCCT were determined from values measured 30 days after AOH relative to baseline (before AOH).

**Results:** In the 60-minute AOH groups, RGC loss varied even when IOP was increased up to 110 mm Hg (36.8%–68.2%). However, for longer durations (90 and 120 minutes), a narrow range of IOP levels (60–70 mm Hg for 90-minute duration; 55–65 mm Hg for 120-minute duration) produced a significant difference in RGC loss, ranging from <25% to >90%. Additionally, loss of YFP-expressing RGCs was comparable to that of total RGCs in the same retinas.

**Conclusions:** Reproducible RGC loss during AOH depends on precise durations and IOP thresholds. In the current study, the optimal choice is an AOH protocol set at 70 mm Hg for a duration of 90 minutes.

**Translational Relevance:** This study can assist in determining the optimal duration and intensity of IOP for the effective utilization of AOH models.

## Introduction

Retinal ischemia/reperfusion (IR) injury is a common cause of visual impairment and blindness, with the final stage marked by the death of retinal ganglion cells (RGCs).<sup>1,2</sup> Acute ocular hypertension (AOH)-induced ocular ischemia serves as a widely used model in retinal ischemia research, acknowledged across various species because of its recoverable and

highly reproducible elevation of intraocular pressure (IOP).<sup>3</sup>

However, the use of diverse animal models and the presence of interspecies variations have resulted in a lack of consistency regarding ischemic tolerance times for RGCs.<sup>1</sup> Notably, some studies reported variable degrees of RGC loss even under the same AOH insult.<sup>4,5</sup> Furthermore, comparing and unifying the extent of RGC loss in AOH injury across different studies is challenging because of variations in animal

species, IOP levels and durations, and experimental techniques.<sup>3–11</sup>

To address this gap, this study aims to determine the extent of RGC loss in response to different magnitudes and durations of AOH using Thy1-YFP-H transgenic mice. The Thy1-YFP-H mouse strain expresses yellow fluorescent protein (YFP) in approximately 0.2% of RGCs under the Thy1 promoter, enabling the visualization of alterations in dendritic trees, cell bodies, and axonal arborization after experimental injury.<sup>10,12–17</sup> This transgenic mouse strain proves particularly well suited for investigating cellular-level details of RGCs, attributed to its non-discriminatory fluorescence across RGC subtypes.

In clinical studies, peripapillary retinal nerve fiber layer (RNFL) thickness is widely used to differentiate eyes affected by glaucoma. For both human and mouse eyes, evaluating RNFL thickness on a circular scan around the optic nerve head proves optimal for assessing RGC damage, because it captures all RGC axons converging toward the optic nerve head in both species.<sup>18,19</sup> However, measuring RNFL thickness in mice is notably more challenging because of their inherently thinner profiles, particularly in damaged retinas. An alternative for evaluating RGC damage is the ganglion cell complex (GCC), which encompasses RGC axons (RNFL) and RGC somas in the ganglion cell layer (GCL). The GCC, being thicker than the RNFL alone, facilitates easier delineation in all eyes.<sup>20</sup>

In this study, the evaluation of RGC loss encompasses both individual cell count and measurements of retinal ganglion cell complex thickness (GCCT), conducted through confocal scanning laser ophthalmoscopy (CSLO) and spectral-domain optical coherence tomography (SD-OCT), respectively.

## Material and Methods

### Animal Preparation

Adult female B6.Cg-Tg(Thy1-YFP)HJrs/J mice (referred to as Thy1-YFP-H, stock no. 003782; Jackson Laboratory, Bar Harbor, ME, USA) aged 11 to 12 months were used in this study. They were housed on a 12-hour light/dark cycle with standard rodent chow and water as desired. All animal operations were approved by the Institutional Animal Care and Use Committee of Zhongshan Ophthalmic Center and complied with the ARVO Statement for the Use of Animals in Ophthalmic and Vision Research.

### Mouse Model of AOH

The protocol for AOH is based on a previous study.<sup>21</sup> In brief, mice were anesthetized with intraperitoneal injection of 1% pentobarbital, and a topical anesthetic (Alcaine; Alcon, Fort Worth, TX, USA) was administered locally for corneal anesthesia. A 34-gauge needle (TN\*3404CCE; Terumo, Tokyo, Japan) was inserted into the anterior chamber and connected to a reservoir filled with balanced salt solution via polyethylene tubing, with the height of the reservoir precalibrated for manometric control of the target IOP.

A total of 31 groups of mice were used, encompassing 10 groups subjected to varying levels of induced IOP, each lasting for three different durations, as well as a sham control group. The 10 target IOP levels were 68 cm (50 mm Hg), 75 cm (55 mm Hg), 82 cm (60 mm Hg), 88 cm (65 mm Hg), 95 cm (70 mm Hg), 102 cm (75 mm Hg), 109 cm (80 mm Hg), 122 cm (90 mm Hg), 136 cm (100 mm Hg), or 150 cm (110 mm Hg), with three to five mice in each group. The duration of IOP elevation was 60, 90, or 120 minutes for each group. Therefore each eye was exposed to a specific combination of pressure and duration of AOH. Randomization was used to subject the animals to different levels of IOP and durations of AOH exposure. Additionally, a sham control group was included, in which five eyes of five mice underwent the same procedure without IOP elevation (13 mm Hg, 120 minutes).

During the entire procedure, all mice exhibited no signs of leakage between the needle and the cornea. Before needle removal, the reservoir was carefully lowered to approximately 13 mm Hg, reflecting the baseline IOP. After the procedure, topical antibiotic ointment (Tobrex; Alcon) was applied to the conjunctival sac. Great care was taken to avoid puncturing the iris, lens, or inner corneal surface during the entire procedure to minimize potential damage to these structures. To ensure the mice's comfort, they were placed on a heating pad during the cannulations.

### In Vivo Imaging

Serial CSLO imaging of YFP-expressing RGCs and SD-OCT imaging of the GCL using Spectralis HRA+OCT (Heidelberg Engineering, GmbH, Heidelberg, Germany) were performed before and 30 days after AOH injury as reported elsewhere.<sup>10,13,14,20,22</sup> The imaging procedures are detailed below.

### CSLO and YFP-Expressing RGC Counting

Serial CSLO imaging of RGCs (Fig. 1) was performed using a 480 nm excitation laser and

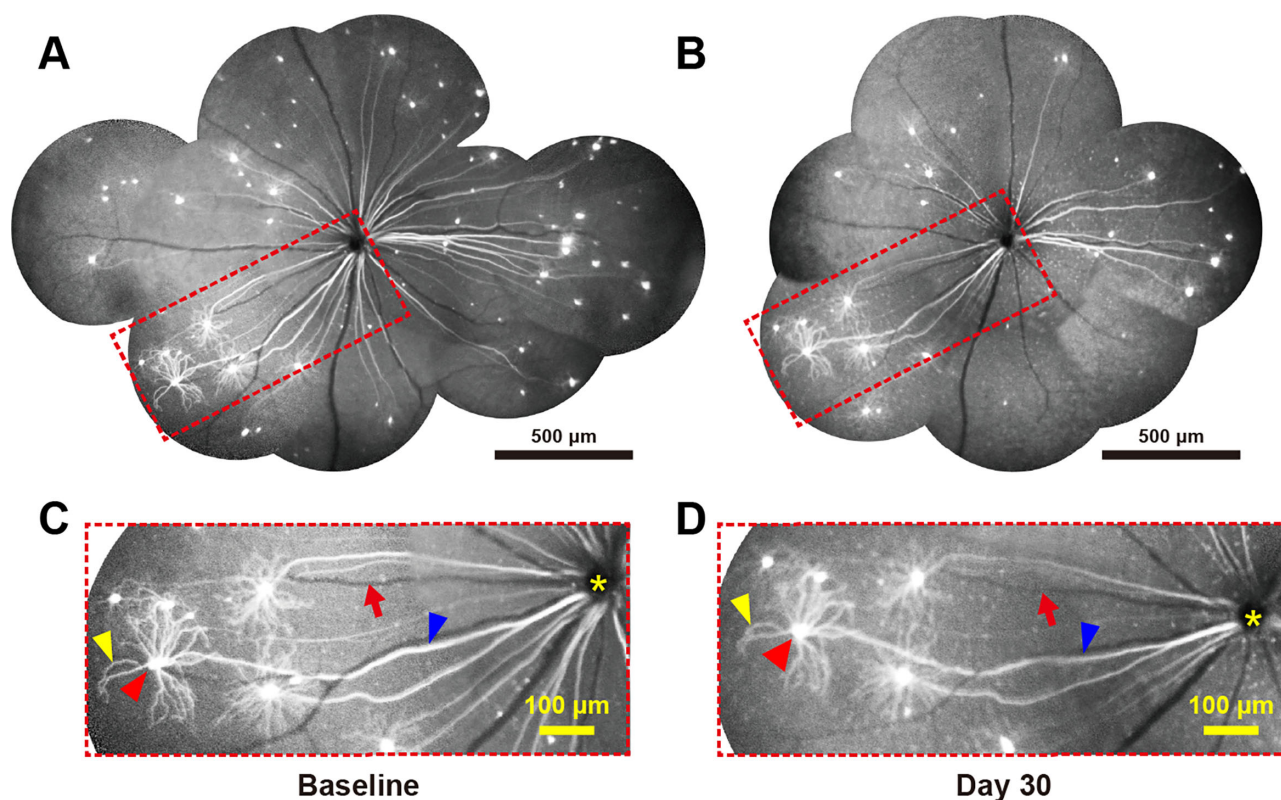


**Figure 1.** Longitudinal retinal photomontages constructed from fundus photographs taken at different gaze angles, depicting the baseline condition (A) and 30 days after inducing AOH (B) by elevating IOP to 90 mm Hg for 60 minutes. Magnified views of the dashed boxes in panels A and B are presented in (C) and (D), respectively. Arrowheads denote different parts of a YFP-expressing RGC, with red, yellow, and blue indicating the cell body, dendrites, and axon, respectively. The red arrow indicates superficial retinal vessels. The degree of YFP-expressing RGC loss was determined using the following formula:  $\text{YFP-expressing RGC loss} = (\text{YFP-expressing RGC count at baseline} - \text{YFP-expressing RGC count at 30 days after AOH}) / \text{YFP-expressing RGC count at baseline}$ .

a 55° lens as previously described.<sup>10,13,14</sup> Briefly, after anesthesia, mice pupils were fully dilated with topical mydriatic agents (Cyclogyl; Alcon). Real-time eye-tracking was used to reduce respiration-induced motion artefacts to a small extent, and 100 images at high-speed mode (768 × 768 pixels) in the same location and focal depth were captured and averaged automatically by Heidelberg software to improve the signal-to-noise ratio. Artificial tears (Hycosan; Ursapharm, Saarbrücken, Germany) were used frequently to maintain the corneal surface moisture and preserve corneal clarity throughout the experiment.

Images were taken with the mice in the following positions: center, mid-periphery, and peripheral area to cover the maximum field of view. To prevent the inclusion of YFP-expressing displaced amacrine and microglial cells that have dendritic arbors similar to RGCs, the assessment was limited to cells with axons originating from their cell bodies and converging toward the optic disc. RGC loss was defined as the complete loss of fluorescence signals as mentioned by

Leung et al.<sup>14</sup> The number of YFP-expressing RGCs was quantified by two investigators who were masked to group allocation, and the average of the two counts was considered as the final number for analysis. The degree of YFP-expressing RGC loss was determined using the following formula:  $\text{YFP-expressing RGC loss} = (\text{YFP-expressing RGC count at baseline} - \text{YFP-expressing RGC count at 30 days after AOH}) / \text{YFP-expressing RGC count at baseline}$ . This formula was used to calculate the percentage reduction in RGC count after AOH injury, with RGC count at baseline serving as a reference point. The resulting value represented the degree of RGC loss as a percentage of the baseline count.

### SD-OCT and GCCT Measurements

After CSLO imaging, the mice immediately underwent SD-OCT imaging to measure peripapillary GCCT using an 870 nm infrared wavelength light source and a 30° lens, as previously described (Fig. 2).<sup>20</sup> The retina was scanned with the peripapillary scanning



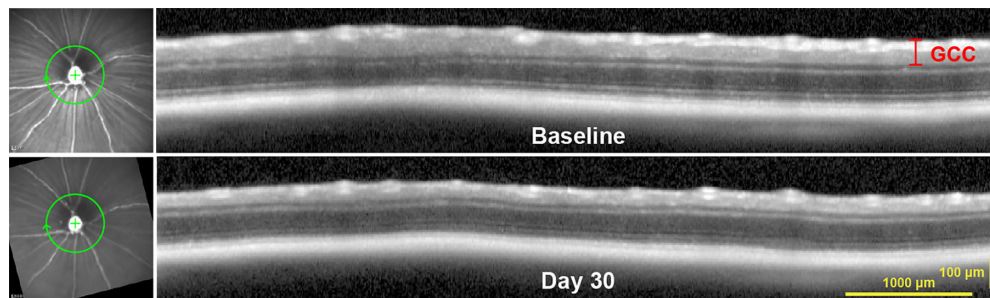


**Figure 2.** Representative peripapillary SD-OCT images of a mouse retina captured at baseline and 30 days after inducing AOH by elevating IOP to 90 mm Hg for 60 minutes (from the same eye as depicted in Figure 1). The GCCT, defined as the combined thickness of the nerve fiber layer, ganglion cell layer, and inner plexiform layer, exhibited a reduction at 30 days after AOH injury, whereas superficial retinal vessels remained visible. The reduction of GCCT was calculated using the following formula: Reduction of GCCT = (GCCT at baseline – GCCT at 30 days after AOH)/GCCT at baseline.

pattern centered at the optic disc under high-speed mode. A real-time eye tracking function was used to reduce speckle noise by averaging 100 frames. The follow-up mode was used to automatically identify and scan the same location repeatedly.

The average GCCT around the optic disc was measured manually by two investigators masked to group allocation with the aid of Heidelberg software, and the two results were averaged for analysis. The reduction of GCCT was calculated using the following formula: Reduction of GCCT = (GCCT at baseline – GCCT at 30 days after AOH)/GCCT at baseline. This formula was used to assess the degree of GCCT loss after AOH injury, with GCCT at baseline serving as a reference point. The resulting value represented the percentage decrease in GCCT from baseline to 30 days after AOH.

## Immunohistochemistry of Retinal Whole-Mounts and Quantification

The eyeballs were enucleated 30 days after AOH injury, fixed in 4% paraformaldehyde for 30 minutes, and then dissected. To prepare the retinas for immunofluorescence staining, they were blocked and permeabilized with a solution of phosphate-buffered saline containing 5% normal donkey serum (Sigma-Aldrich, Munich, Germany), 1% bovine serum albumin (Sigma-Aldrich), and 0.3% Triton X-100 overnight at 4°C. The retinas were subsequently incubated with anti-RNA-binding protein with multiple splicing (RBPMS) antibodies, a pan-RGC marker,<sup>23,24</sup> at a dilution of 1:500 (NBP2-20112; Novus Biologicals, Littleton, CO, USA) for three days at 4°C, followed by incubation with Alexa 555-coupled secondary antibodies (1:1000, 4413S; Cell

Signaling Technology, Danvers, MA, USA) for two hours at  $26^{\circ} \pm 2^{\circ}\text{C}$ . Retinas were then mounted onto glass slides with the nerve fiber layer facing up and four radial incisions were made. Confocal microscopy (LSM880; Carl Zeiss, Oberkochen, Germany) was used to examine the immunohistochemistry of retinal whole-mounts.

To measure the density of RBPMS<sup>+</sup> RGCs, sequential imaging was performed within three square sampling fields (each measuring  $0.4251 \times 0.4251$  mm with a  $20 \times$  objective) from the central, mid-peripheral, and peripheral retina in each quadrant. A total of 12 images were obtained from each retina. In each sampling field, RBPMS<sup>+</sup> cells were manually counted in maximum intensity Z-projections through the ganglion cell layer by two investigators in a masked manner. The cell counts were averaged for each retina. The percentage of RGC loss was calculated as the reduction of RBPMS<sup>+</sup> cell density in each experimental eye compared to the averaged density in sham controls.

## Statistical Analyses

All statistical analyses were performed using Prism version 9.0 (GraphPad, San Diego, CA, USA) and SPSS version 25.0 (SPSS Inc., Chicago, IL, USA). One-way analysis of variance followed by Tukey's post hoc test was used to for comparisons of three and more groups. Pearson's linear regression was applied to assess the strength of any relationship. Nonparametric paired Wilcoxon signed-rank test was used for paired data. Agreement was assessed using intraclass correlation coefficients. *P* values and sample sizes were indicated in figure legends. *P* < 0.05 was considered statistically significant. All results were reported as mean  $\pm$  standard deviation (SD).

Results

Impact of AOH on YFP-Expressing RGC Loss

When ocular hypertension was sustained for 60 minutes, RGC loss increased nonlinearly with increasing IOP. The proportion of lost RGCs was similar across IOPs ranging from 80 to 110 mm Hg (80 mm Hg: 47.95% ± 20.38%; 90 mm Hg: 65.83% ± 10.21%; 100 mm Hg: 55.91% ± 13.63%; 110 mm Hg: 57.78% ± 18.14%; *P* = 0.566). Even when subjected to 110 mm Hg for 60 minutes (Table 1, Fig. 3A), RGC loss remained highly variable (36.84% to 98.04%).

With AOH of 90 minutes, RGC loss was minimal at IOPs ≤60 mm Hg, but sharply increased when IOPs increased from 60 to 70 mm Hg, resulting in a loss of over 90% of RGCs when IOPs were ≥70 mm Hg. The loss of RGCs exhibited the greatest variability when exposed to 65 mm Hg (Table 1, Fig. 3B). A comparable pattern of RGC loss was observed for both the 90-minute (Fig. 3B) and 120-minute (Fig. 3C) durations, despite the IOP threshold being reached at 60 mm Hg during the latter (Fig. 3C). With AOH of 120 minutes, less than 10% of RGCs survived when IOPs were ≥65 mm Hg (Table 1, Fig. 3C).

**Impact of AOH on GCCT Thinning**

GCCT thinning was further evaluated by measuring GCCT 30 days post AOH, which mirrored YFP<sup>+</sup> RGC loss trends (Table 2, Fig. 4). The reduction of GCCT increased nonlinearly with increasing IOP when ocular hypertension was sustained for 60 minutes, as observed in Figure 4A. The percentage of GCCT thinning remained consistent across a range of IOPs from 80 to 110 mm Hg, with values of 30.35% ± 5.64% at 80 mm Hg, 42.95% ± 11.30% at 90 mm Hg, 40.53% ± 23.26% at 100 mm Hg, and 45.05% ± 6.86% at 110 mm Hg (*P* = 0.131). Even when exposed to an IOP of 110 mm Hg for 60 minutes (Table 2, Fig. 4A), the thinning percentage of GCCT remained highly variable, ranging from 37.50% to 50.90%.

When the eyes were exposed to an AOH of 90 minutes, the thinning of GCCT was minimal at IOPs of 60 mm Hg or lower, but sharply increased when the IOPs increased from 60 to 70 mm Hg, resulting in a reduction of over 50% of GCCT when the IOPs were 70 mm Hg or higher. The loss of GCCT showed the greatest variability when the eyes were exposed to an IOP of 65 mm Hg (Table 2, Fig. 4B). Similar reductions in GCCT were observed for both the 90- and 120-minute durations, even though the IOP threshold was reached at 65 mm Hg during the latter. With an AOH

Table 1. The Percentage Reduction in YFP-Expressing RGC Count 30 Days After AOH Injury With Varying Durations and Levels of IOP

Levels of IOP	60 Minutes			90 Minutes			120 Minutes		
	Mean ± SD	Minimum	Maximum	Mean ± SD	Minimum	Maximum	Mean ± SD	Minimum	Maximum
50 mm Hg	0	0	0	0	0	0	0	0	0
55 mm Hg	0	0	0	1.11% ± 1.17%	0	2.33%	5.05% ± 8.75%	0	15.15%
60 mm Hg	2.99% ± 3.62%	0	7.02%	10.65% ± 10.97%	3.33%	23.26%	63.54% ± 55.10%	0	98.04%
65 mm Hg	28.22% ± 22.01%	9.09%	52.27%	62.62% ± 54.36%	0	97.67%	95.45% ± 3.97%	90.32%	100%
70 mm Hg	33.71% ± 31.18%	0	62.07%	98.42% ± 2.17%	96.00%	100%	96.80% ± 2.81%	94.74%	100%
75 mm Hg	39.78% ± 33.15%	2.13%	64.58%	97.18% ± 3.65%	93.06%	100%	98.71% ± 2.24%	96.12%	100%
80 mm Hg	47.95% ± 20.38%	27.27%	74.42%	97.62% ± 4.12%	92.86%	100%	97.92% ± 3.61%	93.75%	100%
90 mm Hg	65.83% ± 10.21%	58.93%	77.55%	96.86% ± 5.44%	90.57%	100%	100%	100%	100%
100 mm Hg	55.91% ± 13.63%	40.58%	66.67%	98.57% ± 1.29%	97.50%	100%	99.09% ± 1.58%	97.26%	100%
110 mm Hg	57.78% ± 18.14%	36.84%	68.33%	100%	100%	100%	96.60% ± 3.38%	93.24%	100%

The degree of RGC loss was determined using the following formula: RGC loss = (RGC count at baseline – RGC count at 30 days after AOH)/RGC count at baseline.

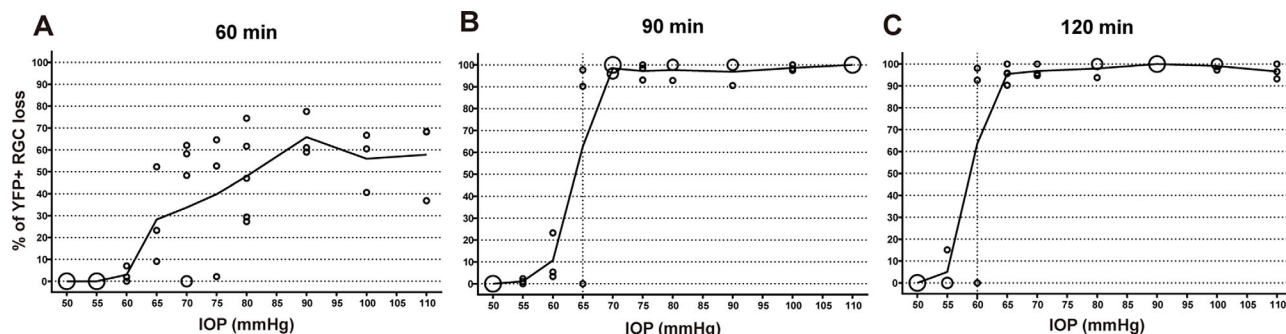


**Figure 3.** The percentage reduction in YFP-expressing RGC count 30 days after AOH induced by a range of IOPs for 60 minutes (A), 90 minutes (B), and 120 minutes (C). The data were collected from three to five mice for each elevated IOP in the three duration groups. The size of the circles represents the number of overlapped observations, with *small open circles* representing a single observation and *large open circles* representing multiple observations.

of 120 minutes, more than 60% of GCCT was lost when the IOP  $\geq 65$  mm Hg (Table 2, Fig. 4C).

### Relationship Between YFP-Expressing RGC Loss and GCCT Thinning

Figure 5 shows the correlation between GCCT reduction (y-axis), measured on a peripapillary circular scan, and YFP-expressing RGC loss (x-axis) on CSLO images. A strong association between YFP-expressing RGC loss and GCCT reduction was found. The correlation coefficient was calculated using Pearson's correlation analysis ( $r = 0.975$ ,  $P < 0.001$ ), with a regression equation of  $Y = 0.641 \cdot X + 0.694$  and a high coefficient of determination ( $R^2 = 0.950$ ).

### Susceptibility of YFP-Expressing RGCs and Total RGCs to AOH Injury

To assess the suitability of Thy1-YFP-H mice as a model for studying AOH-induced RGC loss, we quantified the death rate of YFP-expressing and RBPMS<sup>+</sup> RGCs in the same retinas before and 30 days after AOH insult. Figure 6A1 displays the distribution of RBPMS<sup>+</sup> RGCs on a whole-mount retina derived from an eye exposed to AOH injury, with corresponding magnified views of the central, middle, and peripheral regions shown in Figures 6A2–A4, respectively. Figure 6A5 shows an image of a RBPMS<sup>+</sup> retinal whole-mount from a sham control eye, with magnified views of the central, middle, and peripheral regions shown in Figures 6A6–A8. The density of RBPMS<sup>+</sup> RGCs was highest in the central and medial regions of the retina and lower in the periphery.

We observed a robust correlation between the loss of YFP-expressing RGCs and RBPMS<sup>+</sup> RGCs ( $Y = 1.005 \cdot X - 1.693$ ,  $R^2 = 0.949$ ,  $r = 0.974$ ,

$P < 0.001$ , based on Pearson's correlation coefficient analysis; Fig. 6B), with an intraclass correlation coefficient of 0.974 (95% confidence interval, 0.938–0.989). Moreover, there was no statistically significant difference between the death rates of YFP-expressing RGCs and RBPMS<sup>+</sup> RGCs within the same eye (paired  $t$ -test,  $P = 0.753$ ;  $n = 21$ ; Fig. 6C).

## Discussion

This study used longitudinal in vivo imaging data sets of Thy1-YFP-H transgenic mice to demonstrate RGC loss after AOH with varying IOPs (50, 55, 60, 65, 70, 75, 80, 90, 100, and 110 mm Hg) and durations (60, 90, and 120 minutes). Results showed that RGC loss increased nonlinearly with sustained ocular hypertension for 60 minutes, and similar proportions of RGC loss were observed for IOP elevations between 80 to 110 mm Hg. For AOH lasting 90 minutes, only a small proportion of RGCs ( $<25\%$ ) died when IOPs were  $\leq 60$  mm Hg. However, RGC loss sharply increased when IOPs rose from 60 to 70 mm Hg, reaching more than 90% when IOPs were  $\geq 70$  mm Hg. A similar pattern of RGC loss was observed for the 120-minute duration compared with the 90-minute duration. Additionally, the susceptibility of YFP-expressing RGCs was similar to that of total RGCs, indicating that the Thy1-YFP-H transgenic mouse strain is a reliable model for tracking individual RGC morphology changes and quantifying RGC populations in vivo after AOH insult.

Within this context, we longitudinally studied RGC loss from two perspectives: YFP-expressing RGCs on CSLO and GCCT on SD-OCT. To estimate YFP-expressing RGC loss, we used data obtained from in vivo fundus imaging 30 days after AOH based on previous studies.<sup>4,5,9,10</sup> Notably, this study did not



Table 2. The Percentage Decrease in GCCT From Baseline to 30 Days After AOH With Varying Durations and Levels of IOP

Levels of IOP	60 Minutes			90 Minutes			120 Minutes		
	Duration of AOH			Duration of AOH			Duration of AOH		
	Mean ± SD	Minimum	Maximum	Mean ± SD	Minimum	Maximum	Mean ± SD	Minimum	Maximum
50 mm Hg	−0.23% ± 1.66%	−2.00%	1.30%	−0.20 ± 1.71%	−2.00%	1.40%	1.76% ± 2.04%	0.00%	4.00%
55 mm Hg	0.17% ± 1.16%	−0.90%	1.40%	4.33 ± 1.53%	3.00%	6.00%	8.67% ± 7.23%	4.00%	17.00%
60 mm Hg	−0.47% ± 3.56%	−3.00%	3.60%	9.17% ± 4.86%	5.00%	14.50%	44.04% ± 36.46%	2.00%	67.00%
65 mm Hg	10.16% ± 6.83%	5.48%	18.00%	45.29% ± 31.26%	9.61%	67.89%	63.86% ± 3.45%	59.56%	68.00%
70 mm Hg	12.25% ± 11.65%	−2.00%	25.10%	63.72% ± 2.06%	60.98%	66.67%	61.18% ± 1.06%	60.08%	62.20%
75 mm Hg	19.07% ± 14.04%	3.00%	29.00%	63.24% ± 1.14%	61.94%	64.04%	65.61% ± 2.18%	63.57%	67.90%
80 mm Hg	30.35% ± 5.64%	25.32	36.96%	64.44% ± 2.38%	62.50%	67.09%	67.36% ± 3.23%	64.29%	70.73%
90 mm Hg	42.95% ± 11.30%	35.91%	55.99%	65.07% ± 4.16%	60.71%	69.00%	65.87% ± 2.44%	63.13%	67.82%
100 mm Hg	40.53% ± 23.26%	13.75%	55.71%	66.44% ± 6.30%	60.00%	72.58%	63.55% ± 1.26%	62.17%	64.63%
110 mm Hg	45.05 ± 6.86%	37.50%	50.90%	60.38% ± 5.47%	54.88%	65.82%	62.22% ± 1.58%	60.71%	63.86%

The reduction of GCCT was calculated using the following formula: Reduction of GCCT = (GCCT at baseline – GCCT at 30 days after AOH)/GCCT at baseline.

observe consistent reliability in cell loss at the 60-minute duration, which is commonly used in retinal ischemia/reperfusion models.<sup>3,25</sup> Previous studies have also reported variations in RGC loss with differences in duration and species. Sellés-Navarro et al.<sup>5</sup> observed a duration threshold in rats between 45 and 60 minutes of ischemia, whereas Leung et al.<sup>4</sup> reported a broad spectrum of RGC loss from 14.5% to 79.5% after ischemia for 90 minutes. These variations could be attributed to differences in species, age, and gender and require further investigation to clarify.<sup>3,26–29</sup> Moreover, it is prudent to consider the observed IOP threshold in this study when designing AOH models and conducting related research.

For AOH durations of 120 minutes, we observed threshold effects for RGC loss between 55 to 65 mm Hg, beyond which remarkable RGC loss was observed. Similar to our findings, a previous study reported an “IOP threshold” between 60 and 70 mm Hg for durations longer than 105 minutes in rats, which could induce permanent retinal functional loss.<sup>9</sup> However, it is important to note that AOH with higher IOPs and longer durations may increase the risk of corneal endothelial cell dysfunction, extensive retinal damage, and ocular inflammatory response.<sup>30,31</sup> Thus choosing appropriate IOPs and durations that reach reliable thresholds for RGC loss is crucial in AOH models. The mechanisms underlying threshold effects, such as oxidative stress and activation of microglia/macrophages, require further investigation.<sup>32,33</sup>

Various techniques are available to assess RGC loss, including labeling with neural tracers or immunohistochemistry, calculating ganglion cell layer soma density using adaptive optics-optical coherence tomography, fluorophore expression in RGCs controlled by a gene promoter, and measuring RNFL thickness in postmortem tissues or in vivo imaging.<sup>27,34,35</sup> The development of the Thy1-YFP-H transgenic mouse strain, which expresses YFP in approximately 0.2% of RGCs under the Thy1 promoter, allows for the visualization of changes in dendritic trees, cell bodies, and axonal arborization after experimental injury.<sup>10,12–17</sup> It appears that the Thy1-YFP-H transgenic mouse strain is well suited for studying the cellular-level details of RGCs due to its non-discriminatory fluorescence among RGC subtypes.<sup>15</sup> To date, no studies have simultaneously monitored changes in morphology and number of YFP-expressing RGCs over time. Our study fills this gap and shows that YFP-expressing RGCs are similarly vulnerable to AOH injury as total RGCs, in line with the idea that YFP expression is non-discriminatory among different morphological subtypes of RGCs.<sup>15</sup> We consider

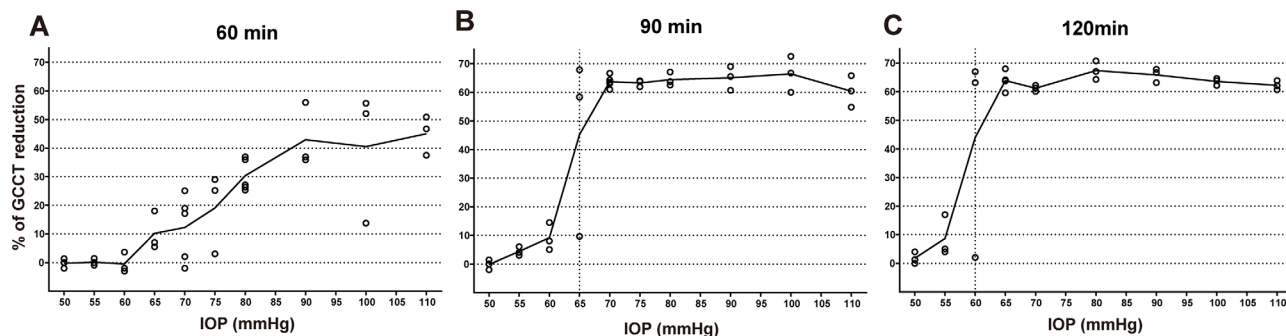


**Figure 4.** The percentage reduction in GCCT 30 days after AOH induced by a range of IOPs for 60 minutes (A), 90 minutes (B), and 120 minutes (C). The data were collected from three to five mice for each elevated IOP in the three duration groups.

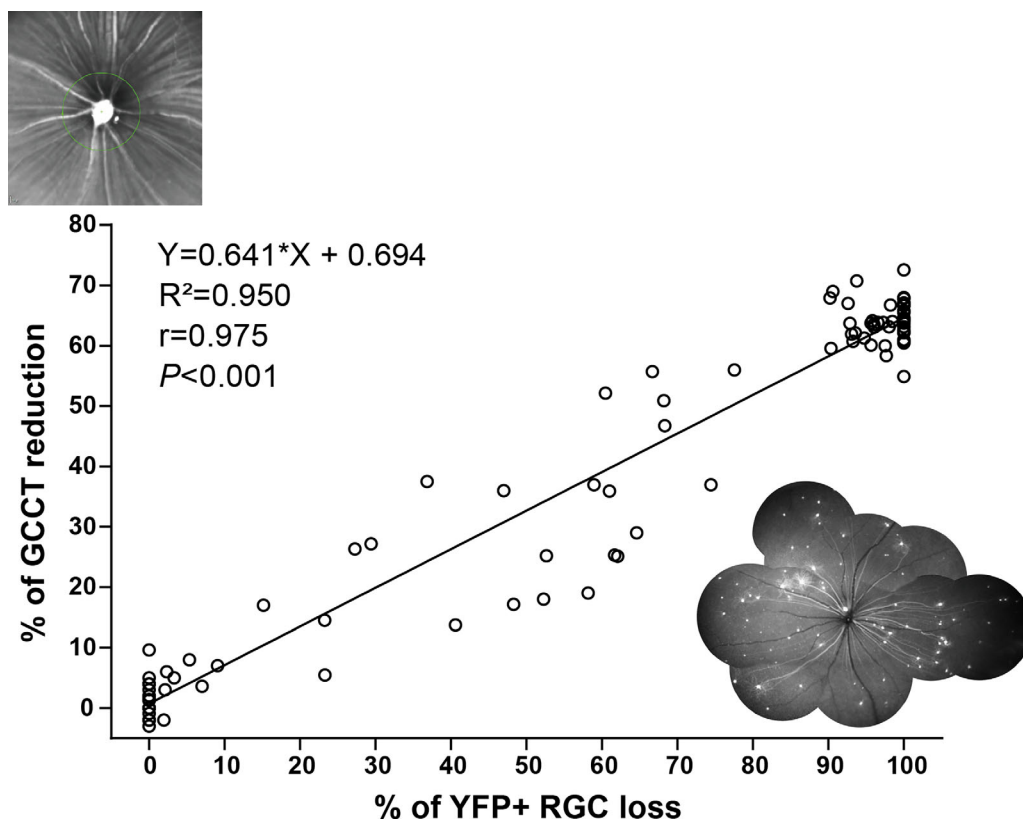


**Figure 5.** The correlation between GCCT reduction, measured on a peripapillary circular scan, and YFP-expressing RGC loss on CSLO images. The proportion of GCCT reduction compared with baseline assessments (y-axis) versus the death rate of YFP-expressing RGCs (x-axis):  $Y = 0.641 \cdot X + 0.694$ ,  $R^2 = 0.950$ ,  $r = 0.975$ ,  $P < 0.001$ , Pearson's correlation coefficient analysis,  $n = 97$ .

the Thy1-YFP-H transgenic mouse strain to be an ideal tool for tracking in vivo morphological changes and estimating total RGC population numbers after AOH, with valuable and reliable features.

This study has potential limitations that could affect the interpretation of the results. Anesthesia-induced reversible lens opacity and cannula-related complications, such as corneal edema and ocular inflammatory responses, are common in experimen-

tal mice and can affect the accuracy of the results. However, precautions were taken to minimize these complications, such as avoiding puncturing the iris, lens, or inner corneal surface and applying artificial tears to prevent corneal drying. Second, in the retinal flat mount experiment, RGC loss predominantly occurs in the peripheral retinas, whereas CSLO primarily scans the central retina. Nevertheless, it is noteworthy that RGCs extend axons from their cell bodies, converging toward the optic disc. Conse-



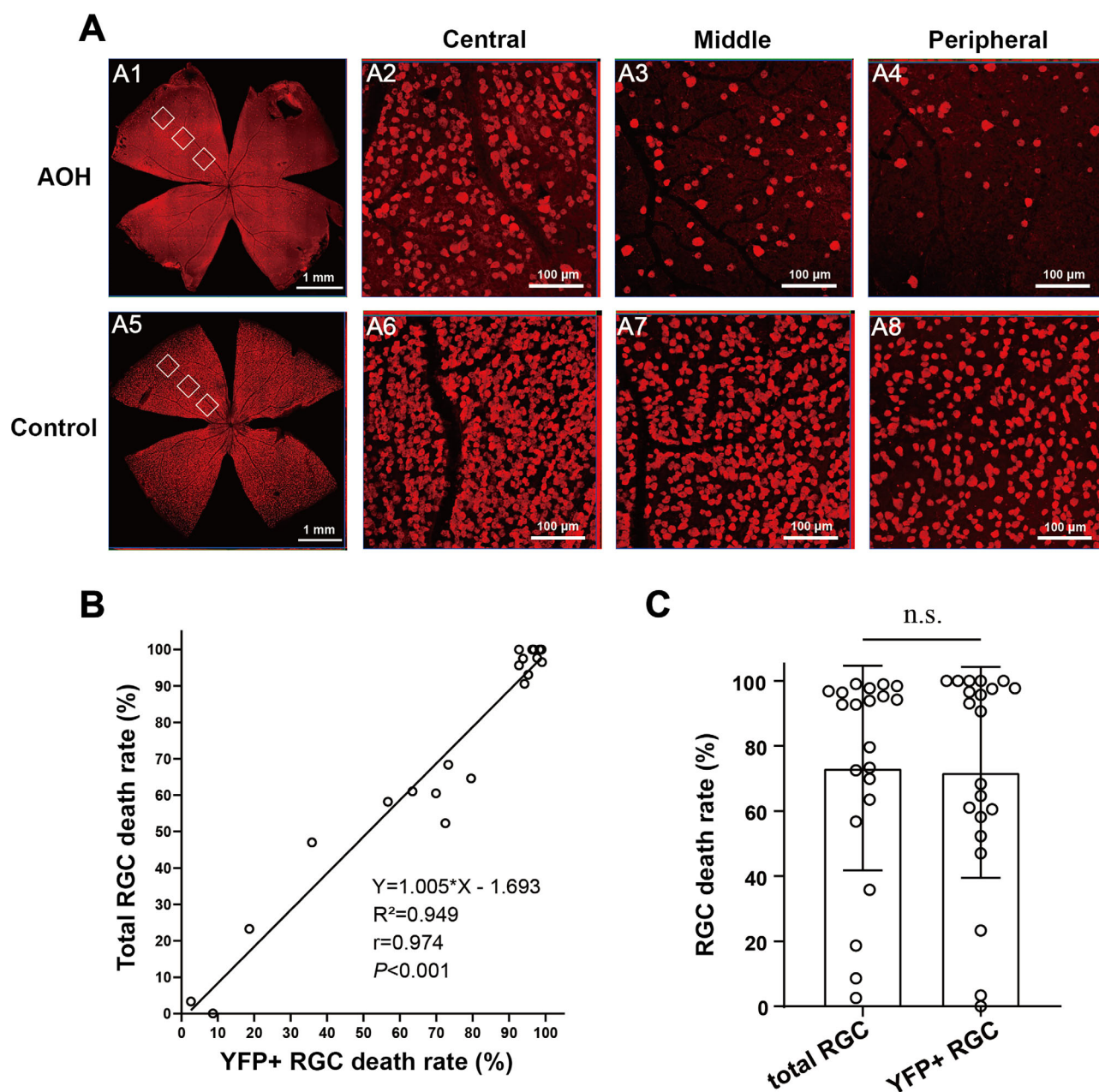


**Figure 6.** Susceptibility of YFP-expressing RGCs and total RGCs to AOH injury. A retinal whole-mount image (**A1**) derived from an eye exposed to AOH injury demonstrated the localization of three representative regions corresponded to central (**A2**), middle (**A3**) and peripheral (**A4**) flat-mounted retinas. Images of another retinal whole-mount (**A5**) derived from a sham control eye and magnified views (**A6–A8**). (**B**) Loss of YFP-expressing RGCs correlated well with total RGC loss. Loss of YFP-expressing RGCs (x-axis) versus that of RBPMS<sup>+</sup> RGCs (y-axis):  $Y = 1.005 \cdot X - 1.693$ ,  $R^2 = 0.949$ ,  $r = 0.974$ ,  $P < 0.001$ , Pearson's correlation coefficient analysis. (**C**) The difference between loss of YFP-expressing RGCs and RBPMS<sup>+</sup> RGCs from the same eyes is not statistically significant (non-parametric paired Wilcoxon signed-rank test,  $P = 0.753$ ,  $n = 21$ ).

quently, despite the narrower scanning field of CSLO compared to the retinal flat mount experiment, the assessment of RGC loss maintains accuracy through the meticulous counting of YFP-expressing RGCs in the Thy1-YFP transgenic mice. Third, it is crucial to acknowledge the disparity between the loss of YFP-expressing RGCs and the reduction in GCCT.

This incongruity may be mainly attributed to the fact that current GCCT measurements include both neuronal and vascular components without differentiation. Previous studies using OCT have demonstrated that retinal vessels in the RNFL can impact thickness measurements,<sup>36,37</sup> resulting in an overestimation of GCCT thickness. Fourth, further research

on non-human primates is needed to validate these findings if they are to be generalized with AOH in humans, because this study was conducted using mouse models.

In conclusion, this study highlights the importance of meeting both duration and IOP thresholds to induce highly reproducible loss of RGCs in animal models of AOH. The findings suggest that future AOH-related research should consider these factors to ensure the reproducibility of their results. Additionally, the results demonstrate that the Thy1-YFP-H transgenic mouse strain is a reliable model for longitudinally characterizing both the overall levels of RGCs and individual RGC morphological changes after AOH insult, because it has similar proportions of loss in YFP-expressing RGCs compared with the total RGC population. These findings provide important insights for understanding the mechanisms underlying RGC loss in AOH and for developing new therapies to prevent or treat this condition.

## Acknowledgments

The authors thank the staff of Laboratory Animal Center and Core Facilities at State Key Laboratory of Ophthalmology, Zhongshan Ophthalmic Center for technical support.

Supported by the Global STEM Professorship Scheme [grant number: P0046113], the Fundamental Research Funds of the State Key Laboratory of Ophthalmology [grant number: 81420108008], and National Natural Science Foundation of China [grant number: 81271037].

Disclosure: **M. Xuan**, None; **W. Wang**, None; **G. Bulloch**, None; **J. Zhang**, None; **J. Ha**, None; **Q. Wang**, None; **J. Wang**, None; **X. Lin**, None; **M. He**, None

## References

- Osborne NN, Casson RJ, Wood JP, Chidlow G, Graham M, Melena J. Retinal ischemia: mechanisms of damage and potential therapeutic strategies. *Prog Retinal Eye Res.* 2004;23:91–147.
- Dvorianchikova G, Degterev A, Ivanov D. Retinal ganglion cell (RGC) programmed necrosis contributes to ischemia-reperfusion-induced retinal damage. *Exp Eye Res.* 2014;123:1–7.
- Pang IH, Clark AF. Inducible rodent models of glaucoma. *Prog Retinal Eye Res.* 2020;75:100799.
- Leung CK, Lindsey JD, Chen L, Liu Q, Weinreb RN. Longitudinal profile of retinal ganglion cell damage assessed with blue-light confocal scanning laser ophthalmoscopy after ischaemic reperfusion injury. *Br J Ophthalmol.* 2009;93:964–968.
- Sellés-Navarro I, Villegas-Pérez MP, Salvador-Silva M, Ruiz-Gómez JM, Vidal-Sanz M. Retinal ganglion cell death after different transient periods of pressure-induced ischemia and survival intervals. A quantitative in vivo study. *Invest Ophthalmol Vis Sci.* 1996;37:2002–2014.
- Crowston JG, Kong YX, Troncone IA, et al. An acute intraocular pressure challenge to assess retinal ganglion cell injury and recovery in the mouse. *Exp Eye Res.* 2015;141:3–8.
- Abbott CJ, Choe TE, Lusardi TA, Burgoyne CF, Wang L, Fortune B. Evaluation of retinal nerve fiber layer thickness and axonal transport 1 and 2 weeks after 8 hours of acute intraocular pressure elevation in rats. *Invest Ophthalmol Vis Sci.* 2014;55:674–687.
- Morrison JC, Cepurna WO, Tehrani S, et al. A period of controlled elevation of IOP (CEI) produces the specific gene expression responses and focal injury pattern of experimental rat glaucoma. *Invest Ophthalmol Vis Sci.* 2016;57:6700–6711.
- Bui BV, Batcha AH, Fletcher E, Wong VH, Fortune B. Relationship between the magnitude of intraocular pressure during an episode of acute elevation and retinal damage four weeks later in rats. *PloS one.* 2013;8:e70513.
- Li ZW, Liu S, Weinreb RN, et al. Tracking dendritic shrinkage of retinal ganglion cells after acute elevation of intraocular pressure. *Invest Ophthalmol Vis Sci.* 2011;52:7205–7212.
- Zhou L, Chen W, Lin D, Hu W, Tang Z. Neuronal apoptosis, axon damage and synapse loss occur synchronously in acute ocular hypertension. *Exp Eye Res.* 2019;180:77–85.
- Feng G, Mellor RH, Bernstein M, et al. Imaging neuronal subsets in transgenic mice expressing multiple spectral variants of GFP. *Neuron.* 2000;28:41–51.
- Henderson DCM, Vianna JR, Gobran J, et al. Longitudinal in vivo changes in retinal ganglion cell dendritic morphology after acute and chronic optic nerve injury. *Invest Ophthalmol Vis Sci.* 2021;62:5.
- Leung CK, Weinreb RN, Li ZW, et al. Long-term in vivo imaging and measurement of dendritic shrinkage of retinal ganglion cells. *Invest Ophthalmol Vis Sci.* 2011;52:1539–1547.

15. Iaboni DSM, Farrell SR, Chauhan BC. Morphological multivariate cluster analysis of murine retinal ganglion cells selectively expressing yellow fluorescent protein. *Exp Eye Res.* 2020;196:108044.
16. Agostinone J, Alarcon-Martinez L, Gamlin C, Yu WQ, Wong ROL, Di Polo A. Insulin signalling promotes dendrite and synapse regeneration and restores circuit function after axonal injury. *Brain.* 2018;141:1963–1980.
17. Lee GH, Stanford MP, Shariati MA, Ma JH, Liao YJ. Severe, early axonal degeneration following experimental anterior ischemic optic neuropathy. *Invest Ophthalmol Vis Sci.* 2014;55:7111–7118.
18. Hood DC, La Bruna S, Tsamis E, et al. Detecting glaucoma with only OCT: implications for the clinic, research, screening, and AI development. *Prog Retinal Eye Res.* 2022;90:101052.
19. Medeiros FA, Zangwill LM, Bowd C, Vessani RM, Susanna R, Jr., Weinreb RN. Evaluation of retinal nerve fiber layer, optic nerve head, and macular thickness measurements for glaucoma detection using optical coherence tomography. *Am J Ophthalmol.* 2005;139:44–55.
20. Nakano N, Ikeda HO, Hangai M, et al. Longitudinal and simultaneous imaging of retinal ganglion cells and inner retinal layers in a mouse model of glaucoma induced by N-methyl-D-aspartate. *Invest ophthalmology & visual science.* 2011;52:8754–8762.
21. Hartsock MJ, Cho H, Wu L, Chen WJ, Gong J, Duh EJ. A mouse model of retinal ischemia-reperfusion injury through elevation of intraocular pressure. *J Vis Exp.* 2016;(113):54065.
22. Li L, Huang H, Fang F, Liu L, Sun Y, Hu Y. Longitudinal morphological and functional assessment of RGC neurodegeneration after optic nerve crush in mouse. *Front Cell Neurosci.* 2020;14:109.
23. Rodriguez AR, de Sevilla Müller LP, Brecha NC. The RNA binding protein RBPMS is a selective marker of ganglion cells in the mammalian retina. *J Comp Neurol.* 2014;522:1411–1443.
24. Kwong JM, Quan A, Kyung H, Piri N, Caprioli J. Quantitative analysis of retinal ganglion cell survival with Rbpms immunolabeling in animal models of optic neuropathies. *Invest Ophthalmol Vis Sci.* 2011;52:9694–9702.
25. Kim BJ, Braun TA, Wordinger RJ, Clark AF. Progressive morphological changes and impaired retinal function associated with temporal regulation of gene expression after retinal ischemia/reperfusion injury in mice. *Mol Neurodegener.* 2013;8:21.
26. Tan C, Hu T, Peng MC, et al. Age of rats seriously affects the degree of retinal damage induced by acute high intraocular pressure. *Curr Eye Res.* 2015;40:300–306.
27. Di Pierdomenico J, Henderson DCM, Giammaria S, et al. Age and intraocular pressure in murine experimental glaucoma. *Prog Retinal Eye Res.* 2022;88:101021.
28. Du M, Mangold CA, Bixler GV, et al. Retinal gene expression responses to aging are sexually divergent. *Mol Vis.* 2017;23:707–717.
29. Kumari R, Astafurov K, Genis A, Danias J. Differential Effects of C1qa ablation on glaucomatous damage in two sexes in DBA/2NNia mice. *PLoS One.* 2015;10:e0142199.
30. Li X, Zhang Z, Ye L, et al. Acute ocular hypertension disrupts barrier integrity and pump function in rat corneal endothelial cells. *Sci Rep.* 2017;7:6951.
31. Palmhof M, Frank V, Rappard P, et al. From Ganglion Cell to Photoreceptor Layer: timeline of deterioration in a rat ischemia/reperfusion model. *Front Cell Neurosci.* 2019;13:174.
32. Yokota H, Narayanan SP, Zhang W, et al. Neuroprotection from retinal ischemia/reperfusion injury by NOX2 NADPH oxidase deletion. *Invest Ophthalmol Vis Sci.* 2011;52:8123–8131.
33. Zhang C, Lam TT, Tso MO. Heterogeneous populations of microglia/macrophages in the retina and their activation after retinal ischemia and reperfusion injury. *Exp Eye Res.* 2005;81:700–709.
34. Mead B, Tomarev S. Evaluating retinal ganglion cell loss and dysfunction. *Exp Eye Res.* 2016;151:96–106.
35. Liu Z, Saeedi O, Zhang F, et al. Quantification of retinal ganglion cell morphology in human glaucomatous eyes. *Invest Ophthalmol Vis Sci.* 2021;62:34.
36. Ye C, Yu M, Leung CK. Impact of segmentation errors and retinal blood vessels on retinal nerve fiber layer measurements using spectral-domain optical coherence tomography. *Acta Ophthalmol.* 2016;94:e211–e219.
37. Hood DC, Fortune B, Arthur SN, et al. Blood vessel contributions to retinal nerve fiber layer thickness profiles measured with optical coherence tomography. *J Glaucoma.* 2008;17:519–528.